

# Self-Optimising Breather Ultrafast Fibre Laser

X. Wu<sup>(1)</sup>, J. Peng<sup>(1)</sup>, S. Boscolo<sup>(2,\*)</sup>, Y. Zhang<sup>(1)</sup>, C. Finot<sup>(3)</sup>, H. Zeng<sup>(1)</sup>

<sup>(1)</sup> State Key Laboratory of Precision Spectroscopy, East China Normal University, Shanghai 200062, China

<sup>(2)</sup> Aston Institute of Photonic Technologies, Aston University, Birmingham B4 7ET, United Kingdom

<sup>(3)</sup> Laboratoire Interdisciplinaire Carnot de Bourgogne, Université de Bourgogne-Franche Comté, 21078 Dijon Cedex, France

\* [s.a.boscolo@aston.ac.uk](mailto:s.a.boscolo@aston.ac.uk)

**Abstract** We demonstrate the self-optimisation of the breather regime in an ultrafast fibre laser through an evolutionary algorithm. Depending on the specified merit function, single breathers with controllable breathing ratio and period, and breather molecular complexes with a controllable number of constituents can be obtained.

## Introduction

Ultrashort fibre oscillators have become essential tools in various important applications. However, many emerging applications require ultrafast lasers with precisely tailored temporal and spectral characteristics, and existing approaches to laser design and development have proven to be inadequate. This inadequacy results from the fact that the pulse generation mechanism in ultrafast lasers usually involves complex nonlinear and dispersive propagation effects, and reaching a desired operating regime depends on precisely adjusting multiple parameters in a high-dimensional space. As user demands become more stringent, the alignment of such systems by trial and error is no longer suitable for laser optimisation. Machine-learning strategies and the use of evolutionary and genetic algorithms have recently shown promising for the design of smart lasers that can tune themselves to desired operating states<sup>[1-11]</sup>. Yet, existing machine-learning tools are mostly designed to target laser generation regimes of parameter-invariant, stationary pulses, while the intelligent excitation of evolving pulse patterns in a laser remains largely unexplored.

Breathing solitons exhibiting periodic oscillatory behavior are attracting considerable research interest in optics by virtue of their connection with a range of important nonlinear dynamics<sup>[12, 13]</sup> and their potential for practical applications, such as in dual-comb spectroscopy<sup>[14]</sup> or the direct generation of high-amplitude ultrashort pulses from a laser cavity<sup>[15, 16]</sup>. Breathers were first studied experimentally in Kerr fibre cavities<sup>[17]</sup> and optical micro-resonators<sup>[18-20]</sup>, and more recently, have also emerged as a ubiquitous mode-locked regime of ultrafast fibre lasers<sup>[21-23]</sup>. In this paper, we implement an evolutionary algorithm (EA) for the self-optimisation of the breather regime in fibre laser cavity mode-locked

through a four-parameter nonlinear polarisation evolution (NPE). We define compound merit functions relying on the characteristic features of the radiofrequency (RF) spectrum of the laser output, which are capable to locate various self-starting breather regimes in the laser, including single breathers with controllable breathing ratio and period, and breather molecular complexes (BMCs) with a controllable number of elementary constituents.

## Experimental setup and principles

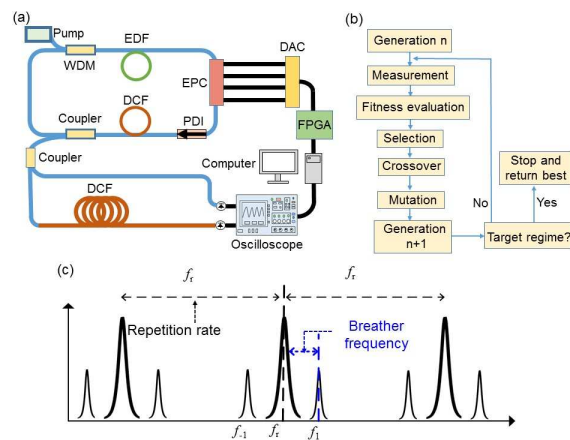


**Fig. 1:** (a) Experiment setup of the self-optimising breather mode-locked laser. (b) Illustration of the EA principle. (c) Sketch of the RF signal under breather mode locking.

The laser (Fig. 1(a)) is an erbium-doped fibre ring cavity with normal dispersion, in which the nonlinear transfer function of the NPE-based mode locking is controlled by an electronically driven polarisation controller (EPC) working together with a polarisation-dependent isolator. The EPC consists of four fibre squeezers oriented at 45° to each other and each controlled by an applied voltage signal and each set of voltages corresponds to a specific polarisation state on the Poincaré sphere. The laser output is split into two ports: a fraction is directly detected by a fast photodiode plugged to a real-time

oscilloscope, while the remaining part is sent through a time-stretch dispersive Fourier transform (DFT) setup<sup>[24]</sup> for spectral measurements. The oscilloscope is connected to a computer that runs the EA and controls the EPC. The EA principle<sup>[25]</sup> is illustrated in Fig. 1(b). In our case, an individual is a laser regime, and the four control voltages applied to the EPC are the genes of the individuals. The process begins with a population of individuals, each comprising a set of randomly assigned genes. The system output is measured for each individual in the generation, evaluated by a user-defined merit function and assigned a score. The EA then creates the next generation by breeding individuals from the preceding generation, with the probability that an individual is selected to be a ‘parent’ based on their score (‘roulette wheel’ selection<sup>[25]</sup>). Two new individuals – children - are created from the crossover of two randomly selected parents. A mutation probability is also specified. This process repeats until the algorithm converges and an optimal individual is produced. Evaluation of the properties of an entire generation of individuals typically takes 3.3 minutes.

A critical factor to the success of a self-optimising laser implementation is the merit function, which must return a higher value when the laser is operating closer to the target regime. To select a breather regime, we need a merit function that discriminates between breather and stationary pulsed operations. The oscillation frequency of the breathers manifests itself as sidebands in the RF spectrum of the laser output, as illustrated in Fig. 1(c), where  $|f_{\pm 1} - f_r|$  represents the breathing frequency, and  $f_r$  and  $f_{\pm 1}$  are the cavity repetition frequency and sideband frequencies, respectively. There are no sidebands located at  $f_{\pm 1}$  when the laser works in a stationary mode locking regime. Therefore, we can design a merit function that exploits the intensity ratio of the central band located at  $f_r$  to the sidebands at  $f_{\pm 1}$ ,

$$C_b = 1 - \frac{\sum_{f=f_r-\Delta}^{f=f_r+\Delta} I(f)}{\sum_{f=f_{-1}}^{f=f_1} I(f)}, \quad (1)$$

where  $\sum_{f=f_r-\Delta}^{f=f_r+\Delta} I(f)$  and  $\sum_{f=f_{-1}}^{f=f_1} I(f)$  are the intensities measured across the the width  $2\Delta$  of the frequency band centred on  $f_r$  and the frequency interval from  $f_{-1}$  to  $f_1$ , respectively. In our experiments, the RF spectrum is obtained directly from the oscilloscope that processes the fast Fourier transform of the laser output intensity recording, and a span of  $f_r \pm 190.72$  KHz is chosen for the measurements. To exclude other laser modes that may also feature sidebands in the RF spectrum, such as relaxation oscillations or noise-like pulse emission, we use the merit function relating to the mode-locked laser operation<sup>[7]</sup>, which is derived from the feature that

mode-locked pulses have a significantly higher intensity than free-running states:

$$C_{ml} = \sum_{i=1}^L I_i / L, \quad I_i = \begin{cases} I_i, & I_i \geq I_{th} \\ 0, & I_i < I_{th} \end{cases} \quad (2)$$

In Eq. (2),  $L$  is the number of laser output intensity points recorded by the oscilloscope ( $L=2^{24}$ , corresponding to a time trace of  $\sim 2700$  cavity round trips),  $I_i$  is the intensity at point  $i$  and  $I_{th}$  is a threshold intensity that noise should not exceed. We can then define the total merit function of the breather mode-locking regime as

$$F_{merit} = \alpha C_{ml} + \beta C_b, \quad (3)$$

where the weights  $\alpha$  and  $\beta$  are determined empirically and set to 40000 and 10, respectively. The search for single-breathing soliton mode locking is implemented here as a three-stage optimisation procedure. The first stage involves scoring each individual against the merit function  $C_{ml}$ , which enables the exclusion of relaxation oscillation regimes, and checking the maximum peak intensity of the pulses to exclude noise-like pulse mode locking. The second stage involves pulse counting to select mode locking at the fundamental repetition frequency. Finally, the individuals passing through the first two stages, are scored against the compound merit function  $F_{merit}$  to exclude stationary pulse states. The inclusion of additional components in the definition of  $F_{merit}$  is the key to achieving advanced control of the characteristics of the breather state, such as tuning of the oscillation period or breathing ratio. Further, the use of  $F_{merit}$  followed by pulse count at a different pump-power level enables the generation of BMCs with an optimised number of elementary constituents.

## Results

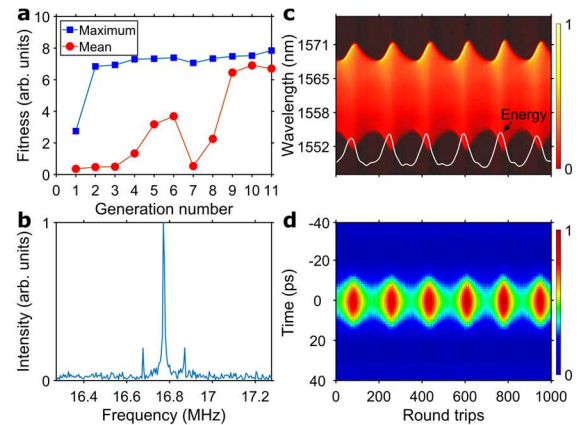


**Fig. 2:** (a) Evolution of the average and maximum merit scores over successive generations, for the merit function given in Eq. (3). (b-d) Characteristics of the optimised state: (b) RF spectrum. (c) DFT recording of single-shot spectra over consecutive cavity round trips. (d) Temporal evolution of the intensity relative to the average round-trip time over consecutive round trips.

In a first series of experiments, we generate single breathers without imposing any additional constraint on the features of the breather solution that is targeted. The pump power is fixed to 70 mW. An example of an optimisation curve is presented in Fig. 2(a), which shows that the best merit score quickly increases and converges to an optimised value after only 2 generations (i.e., after 6 minutes). The average score of the population gradually increases to converge to almost the same value. The spectral and temporal characteristics of the optimal state (Fig. 2(b-d)) confirm the operation of the laser in the targeted mode<sup>[21]</sup>: a RF spectrum exhibiting two symmetrical sidebands around the cavity repetition frequency, and a periodic compression and stretching of the optical spectrum over cavity roundtrips, accompanied by synchronous periodic changes of the pulse energy, peak intensity and pulse duration.

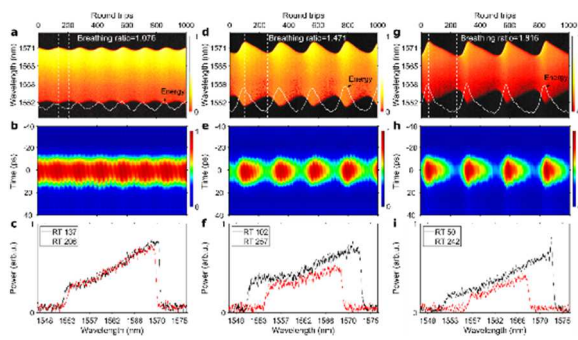


**Fig. 3:** EA optimisation results for breathing solitons with a tunable breathing ratio: dynamics of breathers with (a-c) small, (d-f) moderate and (g-i) large breathing ratios. (a,d,g): DFT recording of single-shot spectra over consecutive cavity roundtrips. (b,e,h): Temporal evolution of the intensity relative to the average round-trip time over consecutive roundtrips. (c,f,i): Single-shot spectra at the round-trip numbers of maximal and minimal spectrum extents within a period.

Since the strength of the frequency sidebands in the RF spectrum is proportional to the breathing ratio (defined as the ratio of the largest to the narrowest width of the pulse spectrum within a period), the latter can be optimised by taking into account the sidebands' strength in the definition of the merit function. Figure 3 shows the spectral and temporal dynamics of three examples of breathers with different breathing ratios that can be generated in the laser cavity by setting corresponding values in the merit function. They refer to the weakest breathing regime found in the cavity, which features a breathing ratio of 1.076, the strongest breathing regime with a breathing ratio of 1.816, and a moderate breathing regime. We have also adapted the merit function to the optimisation of the oscillation period of the breathers, with the results confirming that the designed merit function can indeed be reliably used to tune this feature automatically.

The procedure for the excitation of BMCs, i.e., robust multi-breather bound states that can form

from the interaction of breathers within specific cavity parameter ranges, is not straightforward<sup>[21]</sup>. Here we generate BMCs by using the merit function given in Eq. (3) when the pump power is set to a level that favours multi-pulse self-starting of the laser, and subsequently applying pulse count to control the number of breathers in the established multi-breather states. Considering that the individuals of a population are scored only against the number of breathers constituting the formed multi-breather states, several types of breather-pair molecules with very different dynamics can be accessed. One such example is presented in Fig. 4. The dynamics of the relative phase within the molecule – which is retrieved from the first-order single-shot optical autocorrelation traces computed by Fourier transform of the DFT spectra<sup>[26]</sup> –, feature a pronounced oscillating behavior, indicating that the two breathers continuously exchange energy with each other. At the roundtrip numbers where the phase evolution function has extrema, the two breathers feature equal intensities, and the total energy is highest. In a similar manner to the breather-pair case, the EA allows us to find different bound breather triplets and quadruplets, which are representative of three breather complex categories:  $(M+1)$  and  $(1+M)$  BMCs,  $M=2,3$ , and breather triatomic or tetratomic molecules.

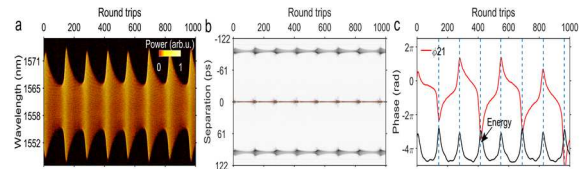


**Fig. 4:** EA optimisation results for an “oscillating-phase” breather-pair molecule. (a) DFT recording of single-shot spectra over consecutive cavity roundtrips. (b) Evolution of the first-order single-shot autocorrelation trace over consecutive roundtrips. (c) Evolution of the phase difference between the two breathers and the energy of the molecule as a function of the roundtrip number.

## Conclusions

We have demonstrated the possibility of using EAs to perform search and optimisation of the breathing soliton regime in a fibre laser cavity. Our work opens novel opportunities for the exploration of highly dynamic, non-stationary operating regimes of ultrafast lasers, such as soliton explosions, non-repetitive rare events and intermittent nonlinear regimes<sup>[27]</sup>. A promising application of the EA approach could be to the emerging multimode fibre laser designs<sup>[28-31]</sup>, in which the vast parameter space makes systematic exploration impracticable, yet ideally suited to optimisation by an EA.

## References

- [1] U. Andral *et al.*, "Fiber laser mode locked through an evolutionary algorithm," *Optica*, vol. 2, pp. 275-278, 2015.

- [2] U. Andral *et al.*, "Toward an autsetting mode-locked fiber laser cavity," *J. Opt. Soc. Amer. B*, vol. 33, pp. 825-833, 2016.
- [3] R. Woodward and E. J. Kelleher, "Towards 'smart lasers': self-optimisation of an ultrafast pulse source using a genetic algorithm," *Sci. Rep.*, vol. 6, 37616, 2016.
- [4] D. G. Winters, M. S. Kirchner, S. J. Backus, and H. C. Kapteyn, "Electronic initiation and optimization of nonlinear polarization evolution mode-locking in a fiber laser," *Opt. Express*, vol. 25, pp. 33216-33225, 2017.
- [5] R. Woodward and E. Kelleher, "Genetic algorithm-based control of birefringent filtering for self-tuning, self-pulsing fiber lasers," *Opt. Lett.*, vol. 42, pp. 2952-2955, 2017.
- [6] A. Kokhanovskiy *et al.*, "Machine learning methods for control of fibre lasers with double gain nonlinear loop mirror," *Sci. Rep.*, vol. 9, 2916, 2019.
- [7] G. Pu, L. Yi, L. Zhang, and W. Hu, "Intelligent programmable mode-locked fiber laser with a human-like algorithm," *Optica*, vol. 6, pp. 362-369, 2019.
- [8] X. Wei, J. C. Jing, Y. Shen, and L. V. Wang, "Harnessing a multi-dimensional fibre laser using genetic wavefront shaping," *Light: Sci. Appl.*, vol. 9, 149, 2020.
- [9] J. Girardot *et al.*, "Autosetting mode-locked laser using an evolutionary algorithm and time-stretch spectral characterization," *IEEE J. Sel. Top. Quantum Electron.*, vol. 26, 1100108, 2020.
- [10] G. Genty *et al.*, "Machine learning and applications in ultrafast photonics," *Nat. Photon.*, pp. 91-101, 2020.
- [11] G. Pu *et al.* "Intelligent control of mode-locked femtosecond pulses by time-stretch-assisted real-time spectral analysis," *Light: Sci. Appl.*, vol. 9, 13, 2020.
- [12] C. Bao *et al.*, "Observation of Fermi-Pasta-Ulam recurrence induced by breather solitons in an optical microresonator," *Phys. Rev. Lett.*, vol. 117, 163901, 2016.
- [13] A. Mussot *et al.*, "Fibre multi-wave mixing combs reveal the broken symmetry of Fermi-Pasta-Ulam recurrence," *Nat. Photon.*, vol. 12, pp. 303-308, 2018.
- [14] P. Liao *et al.*, "Chip-scale dual-comb source using a breathing soliton with an increased resolution," in *Conference on Lasers and Electro-Optics*, San Jose, California, 2018, p. JTh5A.4.
- [15] W. Chang, J. M. Soto-Crespo, P. Vouzas, and N. Akhmediev, "Extreme soliton pulsations in dissipative systems," *Phys. Rev. E*, vol. 92, 022926, 2015.
- [16] W. Chang, J. M. Soto-Crespo, P. Vouzas, and N. Akhmediev, "Extreme amplitude spikes in a laser model described by the complex Ginzburg-Landau equation," *Opt. Lett.*, vol. 40, pp. 2949-2952, 2015.
- [17] F. Leo *et al.*, "Dynamics of one-dimensional Kerr cavity solitons," *Opt. Express*, vol. 21, pp. 9180-9191, 2013.
- [18] M. Yu *et al.*, "Breather soliton dynamics in microresonators," *Nat. Commun.*, vol. 8, 14569, 2017.
- [19] E. Lucas *et al.*, "Breathing dissipative solitons in optical microresonators," *Nat. Commun.*, vol. 8, 736, 2017/09/29 2017.
- [20] D. C. Cole and S. B. Papp, "Subharmonic entrainment of Kerr breather solitons," *Phys. Rev. Lett.*, vol. 123, 173904, 2019.
- [21] J. Peng, S. Boscolo, Z. Zhao, and H. Zeng, "Breathing dissipative solitons in mode-locked fiber lasers," *Sci. Adv.*, vol. 5, eaax1110, 2019.
- [22] T. Xian, L. Zhan, W. Wang, and W. Zhang, "Subharmonic entrainment breather solitons in ultrafast lasers," *Phys. Rev. Lett.*, vol. 125, 163901, 2020.
- [23] Y. Du, Z. Xu, and X. Shu, "Spatio-spectral dynamics of the pulsating dissipative solitons in a normal-dispersion fiber laser," *Opt. Lett.*, vol. 43, pp. 3602-3605, 2018.
- [24] K. Goda and B. Jalali, "Dispersive Fourier transformation for fast continuous single-shot measurements," *Nat. Photon.*, vol. 7, pp. 102-112, 2013.
- [25] M. Mitchell, *An Introduction to Genetic Algorithms*: MIT Press, 1998.
- [26] Z. Wang *et al.*, "Optical soliton molecular complexes in a passively mode-locked fibre laser," *Nat. Commun.*, vol. 10, 830, 2019.
- [27] C. Lapre *et al.*, "Real-time characterization of spectral instabilities in a mode-locked fibre laser exhibiting soliton-similariton dynamics," *Sci. Rep.*, vol. 9, 13950, 2019.
- [28] L. G. Wright, D. N. Christodoulides, and F. W. Wise, "Spatiotemporal mode-locking in multimode fiber lasers," *Science*, vol. 358, pp. 94-97, 2017.
- [29] L. G. Wright *et al.*, "Mechanisms of spatiotemporal mode-locking," *Nat. Phys.*, vol. 16, pp. 565-570, 2020.
- [30] J. C. Jing, X. Wei, and L. V. Wang, "Spatio-temporal-spectral imaging of non-repeatable dissipative soliton dynamics," *Nat. Commun.*, vol. 11, 2059, 2020.
- [31] Y. Guo *et al.*, "Real-time multispeckle spectral-temporal measurement unveils the complexity of spatiotemporal solitons," *Nat. Commun.*, vol. 12, 67, 2021.